Short-range order in Au-Fe alloys studied by high-temperature Mössbauer spectroscopy

Y. Yoshida, F. Langmayr, P. Fratzl, and G. Vogl
Institut für Festkörperphysik der Universität Wien, Strudlhofgasse 4, A-1090 Wien, Austria
(Received 1 August 1988; revised manuscript received 31 October 1988)

Local atomic configurations of iron atoms in $Au_{1-x}Fe_x$ alloys with $x = 0.01, 0.05, 0.15$ are investigated from 300 up to 1100 K using high-temperature Mössbauer spectroscopy. In all alloys a short-range order (anticlustering) tendency is observed. Complementary x-ray small-angle scattering experiments reveal no Fe clusters of the Guinier-Preston-zone type in agreement with the result from Mössbauer experiments. The temperature dependence of the first short-range-order parameter, α_1, obtained from the Mössbauer spectra, is surprisingly weak. A computer simulation shows that, however, the short-range-order can be temperature dependent due to the effect of higher-order correlations, namely third-neighbor Fe-Fe pairs. These higher-order correlations may play an important role for the magnetic properties at low temperature.

I. INTRODUCTION

Au-Fe alloys are well known for their interesting magnetic behavior which does not only depend on the Fe concentration but also on the thermal history of the sample. Magnetic susceptibility[1] and Mössbauer spectroscopy[2] show that in the concentration range near 15 at. % Fe the transition from a paramagnetic to a ferromagnetic state is followed, at very low temperatures, by a second transition to a spin-glass state. No ferromagnetic phase is found at smaller iron concentrations: The paramagnetic state changes directly into a spin glass. It is generally believed that the double magnetic transition near 15 at. % Fe is associated with interacting ferromagnetic spin clusters, which can be observed directly by magnetic neutron small-angle scattering.[3] On the other hand, there is a strong dependence of the magnetic phase diagram on the previous sample treatment at high temperatures[4] and therefore on the atomic order present in the alloy.

Some time ago an investigation of the atomic ordering by diffuse x-ray scattering[5] showed intensity near the $(1\frac{1}{2}0)$ reciprocal-lattice point, which was interpreted as arising from iron-rich platelets in an iron-poor matrix. This model was used by Violet and Borg[6] to interpret their Mössbauer data at low temperatures in terms of the coexistence of two phases with different Fe content. This was the start of a considerable controversy regarding the interpretation of Mössbauer data in the region of the double transition.[7] Additional information on the nature of the atomic ordering in Au-Fe was obtained during the last years, but the results are still controversial: New measurements with diffuse x-ray scattering[8] confirmed the results of Dartyge *et al.*[5] Some authors investigated Au-15 at. % Fe by transmission-electron microscopy and claimed the existence of Fe clusters similar to Guinier-Preston (GP) zones in Al-Cu or Cu-Be.[9] No clusters were, however, observed by Stobbs[10] using high-resolution electron microscopy, even though in electron diffraction patterns of the same samples intensity appeared at the $(1\frac{1}{2}0)$ reciprocal-lattice point. He concluded that this intensity was due to a short-range order (SRO) of the $(1\frac{1}{2}0)$ "special-point" type similar to Au_4Cr, Au_4V, or Ni_4Mo.[11] Consequently the two different iron sites observed by Mössbauer spectroscopy at low temperatures should not be due to the existence of two different phases (iron-rich and iron-poor) but to different local environments of Fe atoms within a single, short-range-ordered phase.[7] Finally a recent study of the magnetic SRO by diffuse neutron scattering[12] showed that, like atomic scattering, magnetic diffuse scattering is also centered at the $(1\frac{1}{2}0)$ point but cannot be entirely attributed to isolated ferromagnetic platelets (GP zones). The authors concluded on some mixture of ordering and clustering.[12]

To gain more insight into the atomic SRO of Au-Fe alloys we have undertaken an investigation using Mössbauer spectroscopy at *high temperatures* in the paramagnetic state of Au-Fe. The starting point was a recent work by Whittle and Campbell[13] who measured the Mössbauer spectra in Au-Fe alloys after quenching from high temperatures. They deduced a negative first SRO parameter indicating "anti-clustering," but the results for the higher temperatures might have been biased by the quenching procedure. To avoid this effect we have performed Mössbauer investigations directly at high temperatures which enabled us to obtain the first SRO parameter up to 1100 K without quenching the sample. Finally, the possible existence of GP zones has been investigated using x-ray small-angle scattering performed on the same sample.

II. EXPERIMENTAL PROCEDURE

The starting materials were Au and ^{57}Fe with $6N$ and $3N$ purity, respectively. Three different specimens with Fe concentrations of 1, 5, and 15 at. % were prepared by using an electron gun under ultrahigh vacuum (10^{-8} mbar). No weight loss was detected after melting, and the concentrations of Fe were checked to an accuracy of ± 0.5 at. % by x-ray diffractometer measurements of the

lattice parameter. Therefore, the nominal Fe concentrations will be used in the following. The specimens were cold-rolled down to 3-μm thickness as appropriate for the use as Mössbauer absorber specimens. The measurements were performed under ultrahigh vacuum (10^{-8} mbar) in a special high-temperature furnace, which has been recently described.[14] The highest temperature in this experiment was 1200 K. During measurements at high temperature the specimen temperature was controlled within ± 1 K. Typical measuring time was between 1 and 3 days per spectrum using a 100 mCi ^{57}Co-in-Rh standard source with a full width at half maximum (FWHM) of 0.12 mm/s.

III. RESULTS

In order to deduce a short-range-order parameter and its temperature dependence from the Mössbauer spectra, both the hyperfine parameters and the Debye-Waller factors for the different atomic configurations of Fe in Au should be well known. For that aim, we first investigated a specimen of Au-5 at. % Fe. The hyperfine parameters obtained for this alloy were then completed by some results from Au-1 at. % Fe and used to perform an analysis of the Mössbauer spectra from Au-15 at. % Fe. By this procedure a consistent set of parameters was obtained for all three alloys. This enabled us to assign the different contributions in the Mössbauer spectra to particular arrangements of the nearest neighborhood of the Mössbauer probe atom. Thus, finally, information about the SRO of Au-Fe was obtained.

A. Fit parameters for $Au_{1-x}Fe_x$

Figures 1(a) and 1(b) show Mössbauer spectra of Au-5 at. % Fe for an as-rolled and an annealed sample, respectively. The spectrum of the as-rolled specimen at room temperature, which is presented at the top of Fig. 1(a), is quite similar to those published in former work.[13,15,16] When the as-rolled sample is heated up the relative intensities of the satellite lines irreversibly decrease at about 450 K, as shown in Fig. 1(a). These satellite lines never reach their original heights in the spectra during all subsequent temperature cycles and therefore characterize the as-rolled state. In no spectrum did we find a six-line component attributable to ferromagnetic iron precipitation, as had been reported by some authors.[17]

We have fitted all spectra using transmission integrals[18,19] with three different components in order to obtain directly an effective thickness, T_A^i, which is expressed by

$$T_A^i = \sigma_0 t_A N F_i f_i \ , \tag{1}$$

where σ_0 is the resonance cross section, t_A the thickness of the absorber, N the total number of resonant absorbing atoms (^{57}Fe) per unit volume, F_i the fraction of absorbing atoms corresponding to the ith component, and f_i the Debye-Waller factor (the recoil-free fraction) for the ith component. We use the transmission-integral fitting because, for a finite thickness of the absorber, the conventional Lorentzian fit may give a wrong value for the fraction due to saturation effects.[18] In addition, for the transmission-integral fit the absorber linewidths of the different components do not depend on the effective thicknesses as in the conventional Lorentzian fit. Therefore, it was possible to keep the linewidths constant for all components in every interaction during the

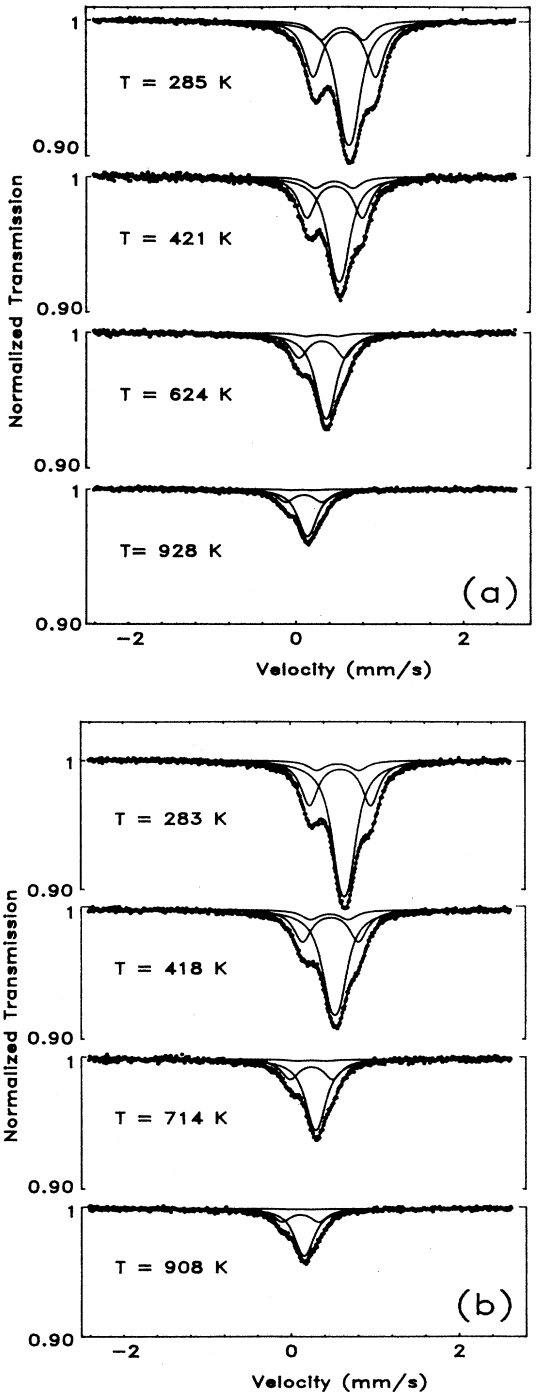

FIG. 1. Mössbauer spectra of Au-5 at. % Fe (a) during increasing temperature (starting with an as-rolled sample) and (b) during decreasing temperature.

transmission-integral fitting. A possible texture effect on the resonance intensities of the doublet[20] can be excluded, because fits using two single lines instead of a doublet yielded always the same intensities for the two lines. Consequently, only symmetric doublets have been used in our fits.

For all three components the effective thickness (a), the linewidth (b), the center shift (c), and the quadrupole splitting (d) are plotted in Fig. 2 as functions of temperature. The solid symbols show the data points for the as-rolled sample and the open symbols show the equilibrium states after annealing at high temperature. The temperature dependence of the total effective thickness, which is drawn by asterisks in Fig. 2(a), can be well described up to 900 K using a Debye model with a Debye temperature of 254 K: Deviations from the Debye model are only observed above 900 K where the linewidth [Fig. 2(b)] starts to increase due to the diffusion of Fe atoms. Such a deviation from the Debye model has been observed in many systems and can be interpreted as an anharmonic effect. From the line broadening above 900 K a diffusion constant of $D_{\mathrm{Fe}}=3.8\times10^{-10}$ cm^2/s at 1121 K can be deduced, which is in good agreement with tracer data.[21] The center shifts for all components [Fig. 2(c)] follow the usual second-order Doppler shift corroborating the fits of the high-temperature spectra, where the same set of components as found for the room temperature spectrum was used.

The typical Mössbauer spectra of Au-1 at. % Fe and Au-15 at. % Fe are shown in Fig. 3. The spectra of Au-1 at. % Fe [Figs. 3(a) and 3(b)] can be fitted using the two dominant components from the spectra of Au-5 at. % Fe. For the fitting of the spectra of Au-15 at. % Fe [Figs. 3(c) and 3(d)] we need a new component with a quadrupole splitting of 0.38 mm/s and an isomer shift of 0.9 mm/s at room temperature in addition to the three components obtained for Au-5 at. % Fe.

B. Debye-Waller factor

In order to discuss the temperature dependence of the relative fraction F_i, we must divide the effective thickness T_A^i [Eq. (1)] by the Debye-Waller factor (DWF) f_i which, in principle, can be different for each component. We have solved that problem in the following way. Comparison of the spectra obtained by heating up an as-rolled sample [Fig. 1(a)] with spectra of an annealed one [Fig. 1(b)] proves that the atomic mobility is significant only above 450 K, where the spectrum shapes start to be identical for the two samples. Therefore, below 450 K the relative fraction F_i cannot change because of absence of diffusion. Consequently, the temperature dependence of T_A^i below 450 K must be entirely attributed to the DWF f_i. From the parallelity of the curves, $\log_{10}(T_A^i)$ versus temperature, below 450 K [see Fig. 2(a)] we finally can conclude that the DWF's are practically the same for all components (as assumed in other work[13]), at least up to 450 K. As there is no discontinuity at 450 K, we shall hardly go wrong assuming that this holds for the whole temperature interval investigated here.

Moreover, it is possible to extract an independent information on the DWF from the temperature dependence of the quadrupole splitting, using a theory of Nishiyama *et al.*[22] In this theory the electric field gradient is expressed as a function of the mean-square lattice displacement $\langle u^2\rangle(T)$. According to this theory, a strongly different $\langle u^2\rangle(T)$ (therefore equivalently different DWF)

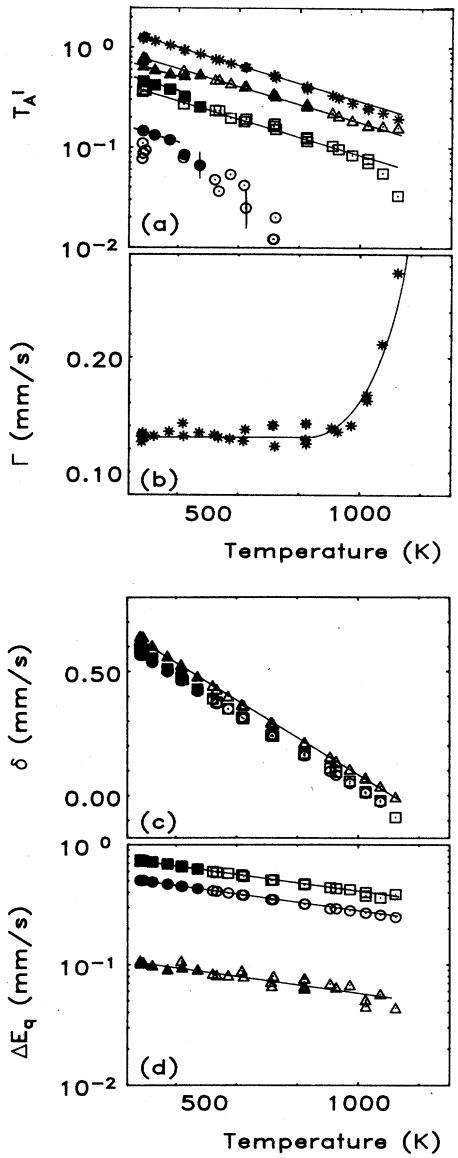

FIG. 2. Fit parameters as functions of temperature, obtained from spectra of Au-5 at. % Fe. Open symbols show data points for a well homogenized sample and solid symbols represent an as-rolled sample during increasing temperature; (a) total effective thickness (*) and effective thickness for monomer (△), dimer (□), and trimer (○) (for assignment see Sec. III C), (b) FWHM of the absorber, (c) center shifts (isomer shifts plus second-order Doppler shifts), and (d) quadrupole splittings in a logarithmic scale. Note that the effective thickness for the trimer becomes very small above 600 K, therefore both the quadrupole splitting and the center shift for the trimer contribution had to be fixed, during fitting above 600 K, to values extrapolated from data points below this temperature.

which might arise, for instance, from a localized motion, would lead to a definitely different temperature dependence of the corresponding electric field gradient. This, however, is not observed in the temperature dependence of the quadrupole splitting [Fig. 2(d)], the curves plotted on a logarithmic scale versus temperature being completely parallel for all components. This gives additional evidence that the DWF can be set equal for all components in a fit.

Therefore, we can set $f_i = f$ in Eq. (1) so that the effective thickness T_A^i for the ith component [Fig. 2(a)] is directly proportional to the relative fraction F_i. Using the normalization condition we can write

$$F_i = T_A^i \Big/ \sum_j T_A^j \ .$$

The fractions F_i are plotted versus temperature in Fig. 4 for the main line [4(a)] and the two doublet contributions [4(b) and 4(c)] for an as-rolled Au-5 at. % Fe sample and one annealed at high temperatures.

C. Assignment of the Mössbauer lines

The concentration dependence of the fit-parameters are shown in Fig. 5; 5(a) presents Debye temperature, 5(b) absorber line width, 5(c) isomer shift, and 5(d) quadrupole splitting, the three latter at room temperature. It is clear from the figure that both the isomer shifts and the quadruple splittings for the three components do not depend on the iron concentration. This implies that the corresponding components obtained in the fits for the three alloys must describe the same local arrangements in the vicinity of the Mössbauer probe atom. For the assignment, therefore, we assume that the quadrupole splitting and the isomer shift for a component are mainly determined by the nearest-neighbor (NN) Fe configuration, the Mössbauer effect being a "short-sighted" method. Fe atoms on the further neighbor shells only affect the spectrum by way of line broadening. Such line broadening can be seen, in fact, in Fig. 5(b). Other than NN

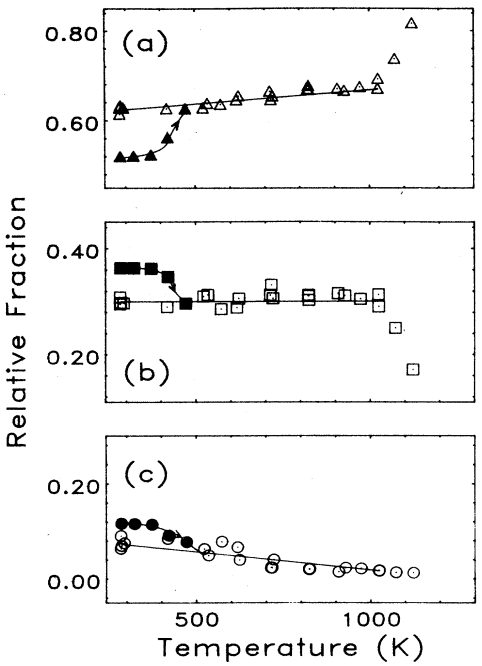

FIG. 4. Relative fractions of temperature obtained from measurements of Au-5 at. % Fe; (a) monomer, (b) dimer, and (c) trimer (for assignment see Sec. III C). Open and solid symbols are for a well homogenized and an as-rolled sample, respectively.

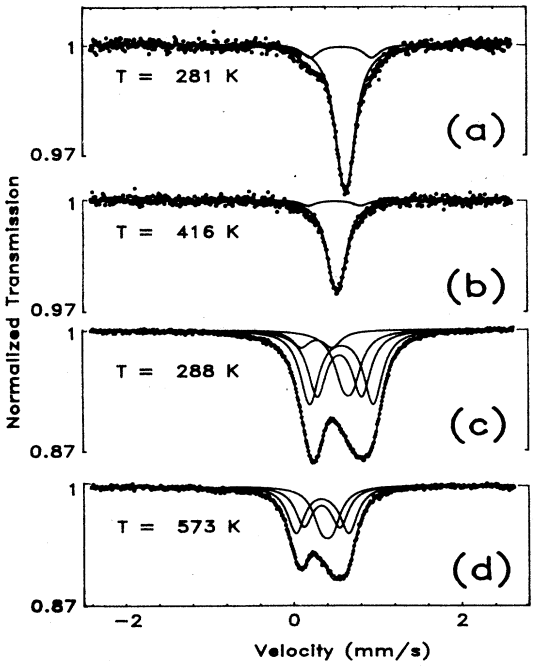

FIG. 3. Typical Mössbauer spectra of Au-1 at. % Fe [(a) and (b)] and Au-15 at. % Fe [(c) and (d)] during increasing temperature starting from the as-rolled state.

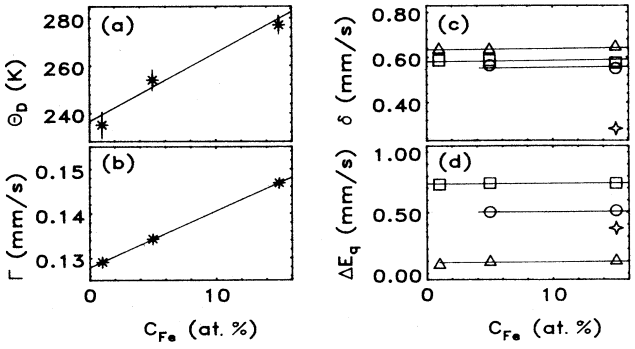

FIG. 5. Concentration dependence of (a) Debye temperature, (b) FWHM for absorber (equal to sample), (c) isomer shifts, and (d) quadrupole splittings [(b), (c), and (d) at room temperature]. △, monomer; □, dimer; ○, trimer; and ✧, quadrumer.

configurations, like, for instance, next-nearest-neighbor (NNN) Fe pairs, which could, in principle, induce independent components in the spectra, are excluded because a strong concentration dependence of the hyperfine parameters would be expected in that case.

Now we can assign all components to particular configurations of the environment of the Mössbauer atom; in a first step, we only consider the components in the spectra of Au-5 at. % Fe. In case of random distribution of Fe atoms in the Au matrix, the most significant configurations of Fe in the Au-5 at. % Fe would be monomers (Fe atoms surrounded by Au only), dimers, trimers, and quadrumers (corresponding to 1, 2, and 3 Fe atoms in the NN shell, respectively) with the appearance probabilities of 0.54, 0.34, 0.10, and 0.02, respectively. Typical clusters are shown in Fig. 6.

Comparing the measured fractions in Au-5 at. % Fe with these values, we assign the main line with a small nonresolved quadrupole splitting of 0.1 mm/s to "monomer Fe" (no Fe atom on the NN sites), the doublet with a quadrupole splitting of 0.72 mm/s to "dimer Fe" (one Fe atom on the NN sites), and another smaller doublet to "trimer Fe" (two Fe atoms on the NN sites).

In the spectra of Au-15 at. % Fe an additional doublet appears when compared to Au-5 at. % Fe. Considering again the random distribution of Fe atoms in the Au lattice, the fourth-frequent component is a quadrumer (see Fig. 6). In fact, the random appearance probabilities for monomer, dimer, trimer, quadrumer, and other (higher-order) clusters in Au-15 at. % Fe are 0.14, 0.30, 0.29, 0.17, and 0.09, respectively. Since the fourth component has no significant distribution of hyperfine parameters, this component also seems to correspond to a unique atomic configuration, probably the quadrumer sketched in Fig. 6.

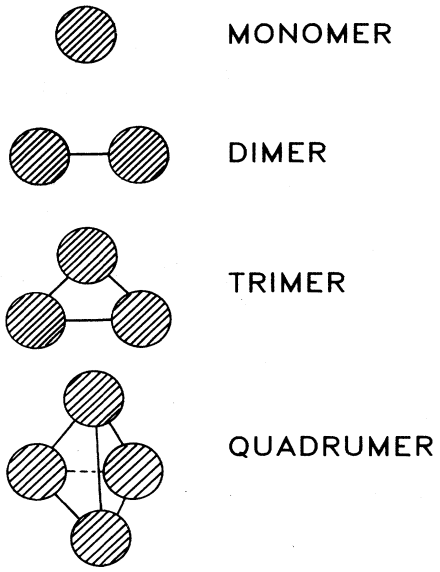

FIG. 6. Sketches for the elementary Fe clusters used in the fits. The bond lengths are all equal to the NN distance.

D. Short-range ordering

The spectrum of the as-rolled Au-5 at. % Fe specimen can be well described by random distribution of Fe atoms in Au. Above 420 K the relative fraction of the monomer increases, and both the fractions of the dimer and the trimer decrease, showing an anticlustering tendency (SRO). This can be directly seen in the spectra [Fig. 1(a)] in that the resonance intensities of the satellite lines at both sides of the main line decrease. In the case of Au-15 at. % Fe the quadrumer line disappears completely above 450 K [Fig. 3(d)] and all subsequent spectra can be well fitted by three components only (monomer, dimer, and trimer), also suggesting SRO in the thermal equilibrium state.

Whittle and Campbell[13] found for the same concentration of iron (5 at. %) either *clustering* in an as-rolled specimen or *atomic SRO* after annealing at about 473 K. The latter agrees rather well with our results from the thermal equilibrium state, i.e., all spectra above 450 K. We never, however, find clustering. We think that the reason for this discrepancy might be that the fits performed by Whittle and Campbell[13] are not quite correct because of the conventional Lorentzian fit which they have used. Effectively when we use a Lorentzian fit for our spectra, we also obtain a clustering tendency for the as-rolled sample (i.e., a smaller fraction for the monomer), which, however, disappears when transmission-integral fitting is used. This seems to be due to a saturation effect which yields apparently a smaller resonance intensity for a component with a larger effective thickness, T_A^i.

The first SRO parameter (α_1) can be written

$$\alpha_1=(z_1-c)/(1-c) .$$

Here z_1 means an average concentration of iron atoms in the NN shell, and c the average concentration of iron atoms in the whole sample. With F_i the relative fraction of Fe atoms having i NN Fe atoms (remember that F_0 corresponding to the monomer fraction, F_i to the dimer fraction, etc.), we obtain

$$z_1=\tfrac{1}{12}\sum_i iF_i .$$

In our case, a contribution from clusters greater than quadrumers cannot be seen, so that $f_i=0$ for $i\geq 4$. The values of the first SRO parameters obtained from the different specimens are summarized in Fig. 7 as functions of temperature. Surprisingly, the temperature dependences of the SRO parameters are very weak for all alloys investigated. The implications of this result will be discussed in the next chapter.

Above 900 K the monomer fraction increases strongly accompanying the disappearance of the dimer in the temperature range where the diffusion line broadening can be clearly observed [Fig. 2(b)]. This interesting finding must result from a dynamical dissociation and association process of Fe atoms within the life time of the 14.4 keV excited state of ^{57}Fe (100 ns). Therefore, we cannot take into account the T_A^i values above 900 K for the interpre-

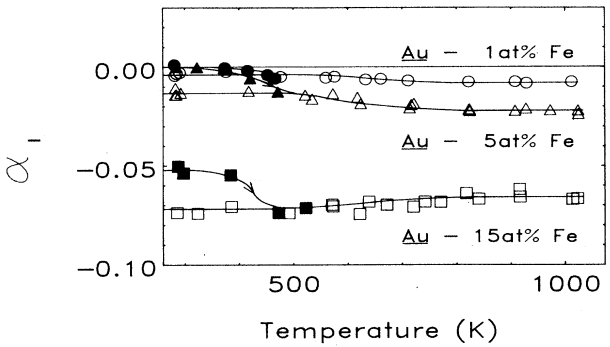

FIG. 7. Temperature dependence of the first SRO parameter α_1 for Au-1 at. % Fe, Au-5 at. % Fe, and Au-15 at. % Fe. Open symbols are for well-homogenized samples, the solid symbols for as-rolled samples all during increasing temperature.

tation in terms of the SRO. The details will be investigated in a forthcoming paper.[23]

E. X-ray small-angle scattering

From the Mössbauer-spectroscopy results we found a tendency toward anticlustering in Au-Fe alloys. In contradiction, however, the existence of Guinier-Preston (GP) zones has been suggested by some authors.[8,9] To test this possibility additional x-ray small-angle scattering experiments have been carried out with one of the samples used before in the Mössbauer experiment.

A point-focus camera mounted on a 12-kW rotating-anode generator providing Mo-$K\alpha$ radiation has been used. We investigated a Au-15 at. % Fe sample quenched from 573 K after slow cooling from 1100 K (in order to get maximum amount of order) and for comparison also as an as-rolled sample. Both times we found a completely flat intensity (Fig. 8) in the range of wave-vector transfer q between 0.04 and 0.3 Å^{-1}, this intensity being essentially due to Au-L fluorescence. Since the strongly q-dependent intensity from platelets similar to GP zones in Al-Cu (Ref. 24) would have been clearly detectable if existent, we conclude that x-ray small-angle scattering yields no evidence for GP-zone formation.

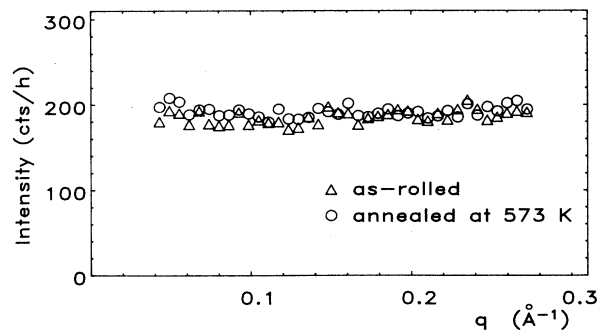

FIG. 8. X-ray small-angle scattering from Au-15 at. % Fe after annealing at 573 K and in the as-rolled state.

IV. DISCUSSION

For all Au-Fe alloys investigated here the first SRO parameter is negative, as is seen in Fig. 7, and shows therefore a tendency towards anticlustering. This is consistent with the Mössbauer investigation on quenched alloys.[13] Regarding the value of α_1, as-rolled samples have a SRO state closer to random distribution (solid symbols in Fig. 7). Only when atomic mobility starts to be significant above 450 K the SRO parameter reaches a value corresponding to equilibrium states (open symbols in Fig. 7).

The temperature dependence of α_1 appears to be surprisingly small. In principle one would expect that α_1 approaches zero for very high temperatures. This tendency does clearly not appear on the data in Fig. 7. Such a result has also been obtained in the study on quenched alloys[13] and has then been interpreted as an effect due to quenching. The authors even concluded that the diffusion coefficient must be considerably enhanced in these alloys, so that SRO may appear *during* the quench. From the high-temperature measurements we can now exclude all effects due to quenching. In addition the diffusion constant of Fe in Au as determined directly from Mössbauer-line broadening [Fig. 2(b)] yields $D_{\mathrm{Fe}} \approx 3.8 \times 10^{-10}$ cm^2/s at 1121 K in agreement with tracer data,[21] indicating that no fast jump mechanism[25] operates in this system and that the Fe diffusion can be described by the usual vacancy mechanism. Therefore the anomalous temperature dependence of α_1 really corresponds to equilibrium states. Nevertheless, the strong influence of the annealing temperature on the magnetic double transition at low temperature[4] indicates that the SRO must be significantly temperature dependent. In the following we shall try to remove this apparent contradiction taking into account the particular features of the $(1\frac{1}{2}0)$ "special-point" ordering.

First our x-ray small-angle scattering measurements exclude the formation of GP zones in quenched samples as recently proposed for Au-Fe alloys.[8,9] Consequently, the intensity around the $(1\frac{1}{2}0)$ point observed by scattering methods[5,10,12] is most likely not due to clusters but to a special-point SRO as proposed by Stobbs.[10] Fits to this type of SRO intensity in other alloys[26] show that the most sensitive SRO parameters are higher-order parameters but not the first one; this is related to the relatively low symmetry of the $(1\frac{1}{2}0)$ point. Starting with SRO parameters published for a typical $(1\frac{1}{2}0)$ special-point alloy[26] we have generated two sets of SRO parameters. The first parameter was both times fixed to the same value of $\alpha_1 = -0.07$, in agreement with α_1 as received from Fig. 7, and only the further SRO parameters were varied. We receive SRO peaks at $(1\frac{1}{2}0)$ with quite different heights. The corresponding intensity contours are shown in Fig. 9. From this picture it appears clearly that an important change in SRO can occur without affecting the first SRO parameter α_1.

In $(1\frac{1}{2}0)$ special-point alloys[26,11] the SRO parameter α_3 corresponding to the third-neighbor distance $[(1\frac{1}{2}\frac{1}{2})$ in cubic indices] is significantly positive; therefore, we suggest that also in the case of Au-Fe a third-neighbor Fe-Fe

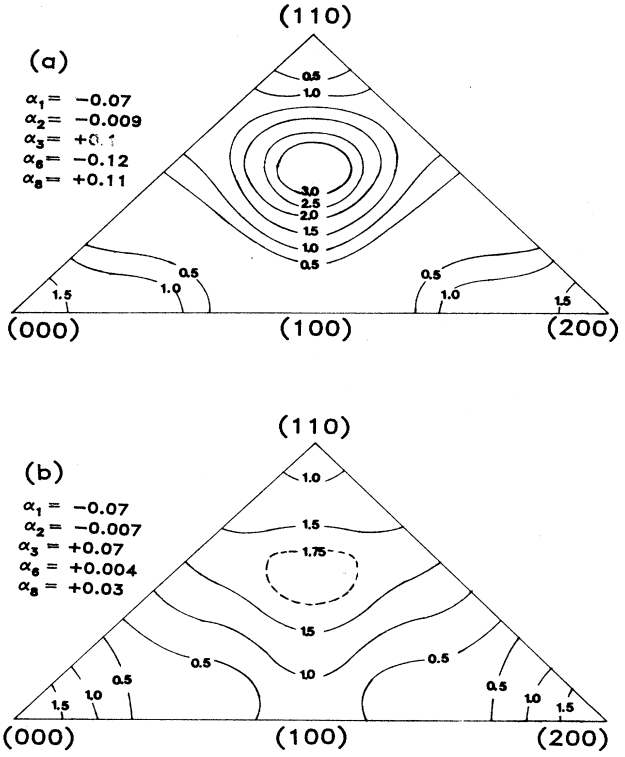

FIG. 9. Calculated isointensity contours of diffuse scattering using the values for the SRO parameters given in the inset. Values for SRO parameters not indicated have been taken as zero. Note that $\alpha_1 = -0.07$ in (a) and (b) in agreement with the SRO parameter obtained for Au-15 at. % Fe (Fig. 7).

correlation might be important. It will probably be this correlation and higher ones that are responsible for the magnetic properties at low temperature, because the first SRO parameter α_1 has been shown to be practically temperature independent by the present high-temperature Mössbauer-spectroscopy investigation.

V. CONCLUSION

Mössbauer spectroscopy is a "short-sighted" method which is particularly sensible for nearest-neighbor interactions. It can therefore be used—as has been undertaken in this work—to determine the first short-range order (SRO) parameter α_1. For the first time Mössbauer spectroscopy has been applied to study SRO in samples not quenched from high temperatures but at temperatures between room temperature and 1100 K. To extract SRO parameters from high-temperature data, particular attention has to be paid to the temperature dependence of the Debye-Waller factor. A careful analysis in the present case shows that the Debye-Waller factors can be taken equal for all components in the Mössbauer spectrum, so that the determination of the SRO parameters is straightforward.

The striking result is that the first SRO parameter α_1 is negative and practically independent of temperature for all investigated alloys (1, 5, and 15 at. % Fe). The negative first SRO parameter is in contradiction to some other work, where a tendency towards clustering is reported,[5,8,9] but supports the assumption that the SRO is of the $(1\frac{1}{2}0)$ special-point type.[10,11] This is confirmed by x-ray small-angle scattering on the same samples as used in the Mössbauer-spectroscopy investigation: no evidence for cluster formation is found.

The surprising fact that α_1 is nearly independent of temperature has been reported in the past[13] for quenched samples and ascribed to the installation of order during the quench, due to very fast diffusion. Our measurements now prove that quenching is *not* the reason for the independence of α_1 from temperature. This independence—on the first view—is in contradiction to the fact that the magnetic phase diagram of quenched Au-Fe strongly depends on the heat treatment before the quench,[4] indicating a strong temperature dependence of the atomic order. We interpret this apparent contradiction in the following way: It is *not* the first SRO parameter α_1 which determines the phase diagram, but SRO is rather due to higher-order correlations. We show by a simulation that variation in α_i (with $i > 1$) while α_1 is kept constant can indeed lead to a quite different amount of SRO. As the SRO parameter α_3 is significantly positive for SRO of the $(1\frac{1}{2}0)$ type, we finally suggest that third-neighbor Fe-Fe pairs could eventually be responsible for the interesting features of the magnetic phase diagram.

ACKNOWLEDGMENTS

We are highly indebted to Dr. K. Grabisch, C. Franke, and H. Baier (Hahn-Meitner-Institut, Berlin) for their help during sample preparation. P. Seebacher and P. Willbacher are greatly acknowledged for experimental help. We thank E. Fössleitner for help with the manuscript. This work was supported in part by "Fonds zur Förderung der Wissenschaftlichen Forschung," Project No. P6733P.

[1]B. R. Coles, B. V. B. Sarkissian, and R. H. Taylor, Philos. Mag. B **37**, 489 (1978).
[2]R. A. Brand, J. Lauer, and W. Keune, Phys. Rev. B **31**, 1630 (1985); I. A. Campbell, S. Senoussi, F. Varret, J. Teiller, and A. Hamzic, Phys. Rev. Lett. **50**, 1615 (1983).
[3]A. P. Murani, Phys. Rev. Lett. **37**, 450 (1976); A. P. Murani, Phys. Rev. B **28**, 432 (1983).
[4]W. Abdul-Razzaq, J. S. Kouvel, and H. Claus, Phys. Rev. B **30**, 6480 (1984).
[5]E. Dartyge, H. Bouchiat, and P. Monod, Phys. Rev. B **25**, 6995 (1982).
[6]C. E. Violet and R. J. Borg, Phys. Rev. Lett. **51**, 1073 (1983).

[7]P. Monod and I. A. Campbell, Phys. Rev. Lett. **52**, 2096 (1984); R. A. Brand and W. Keune, *ibid.* **52**, 2097 (1984); C. E. Violet and R. J. Borg, *ibid.* **52**, 2098 (1984).
[8]C. Marsh, S. Polat, and Haydn Chen, Scr. Metall. **21**, 619 (1987).
[9]C. P. Ju, C. M. Wayman, and Haydn Chen, Scr. Metall. **21**, 59 (1987).
[10]W. M. Stobbs, Phys. Status Solidi A **91**, 69 (1985).
[11]W. M. Stobbs and S. H. Stobbs, Philos. Mag. B **53**, 537 (1986).
[12]J. W. Cable, G. Parette, and Y. Tsunoda, Phys. Rev. B **36**, 8467 (1987).
[13]G. L. Whittle and S. J. Campbell, J. Phys. F **15**, 693 (1985).
[14]A. Heiming, K. H. Steinmetz, G. Vogl, and Y. Yoshida, J. Phys. F **18**, 1491 (1988).
[15]M. S. Ridout, J. Phys. C **2**, 1258 (1969).
[16]B. Window, Phys. Rev. B **6**, 2013 (1972).
[17]G. L. Whittle, R. Cywinski, and P. E. Clark, J. Phys. F **10**, L311 (1980).
[18]S. Margulies and J. R. Ehrmann, Nucl. Instrum. Methods **12**, 131 (1961).
[19]G. K. Shenoy, J. M. Friedt, H. Maletta, and S. L. Ruby, *Mössbauer Effect Methodology,* edited by I. J. Gruvermann, W. Seidel, and D. K. Deiterky (Plenum, New York, 1974), Vol. 9, p. 277.
[20]U. Gonser, in *Microscopic Methods in Metals,* edited by U. Gonser (Springer, Berlin, 1986), p. 435.
[21]D. N. Duhl, K. Hirano, and M. Cohen, Acta Metall. **11**, 1 (1963).
[22]K. Nishiyama, F. Dimmling, Th. Kornrumpf, and D. Riegel, Phys. Rev. Lett. **37**, 357 (1976).
[23]Y. Yoshida, F. Langmayr, P. Fratzl, and G. Vogl (unpublished).
[24]T. Sato, T. Murakami, Y. Amemiya, H. Hashizume, and T. Takahashi, Acta Metall. **36**, 1335 (1988).
[25]Y. Yoshida, W. Miekeley, W. Petry, R. Stehr, K. H. Steinmetz, and G. Vogl, Mater. Sci. Forum **15-18**, 487 (1987).
[26]B. Chakravarti, E. A. Starke, Jr., C. J. Sparks, and R. O. Williams, J. Phys. Chem. Solids **35**, 1317 (1974).